**PAPER** • **OPEN ACCESS**

# Electrospinning and antimicrobial properties of PAN-$Cu_2O$/ZnO nanofibers from green peel extracts

To cite this article: Enyioma C Okpara *et al* 2023 *Mater. Res. Express* **10** 035001



Materials Research Express

PAPER

# Electrospinning and antimicrobial properties of PAN-$Cu_2O$/ZnO nanofibers from green peel extracts

**Enyioma C Okpara**[1,2], **Stephen A Akinola**[3] **and Omolola E Fayemi**[1,2,*]

[1] Department of Chemistry, School of Physical and Chemical Sciences, Faculty of Natural and Agricultural Sciences, North-West University (Mafikeng Campus), Private Bag X2046, Mmabatho 2735, South Africa
[2] Material Science Innovation and Modelling (MaSIM) Research Focus Area, Faculty of Natural and Agricultural Sciences, North-West University (Mafikeng Campus), Private Bag X2046, Mmabatho, 2735, South Africa
[3] Food Security and Safety Niche area, Department of Microbiology, North-West University, Mafikeng Campus, 2735, North-West Province, South Africa
* Author to whom any correspondence should be addressed.

**E-mail:** ebrochima@gmail.com, akinolastephen3@gmail.com **and** Omolola.Fayemi@nwu.ac.za

**Keywords:** electrospinning, green synthesis, antimicrobial, polyacrylonitrile, metal-oxide nanoparticles, nanofibers, nanocomposites

OPEN ACCESS

RECEIVED
5 December 2022

REVISED
8 February 2023

ACCEPTED FOR PUBLICATION
22 February 2023

PUBLISHED
3 March 2023



## Abstract

This study described the antimicrobial activities of waste biomass-mediated $Cu_2O$/ZnO bi-oxide (BiO) nanocomposites; The Orange peels extract (OPE), and lemon peels extract (LPE), were used to synthesize the bioxide nanoparticles (NPs) designated as OPE/BiONPs, and LPE/BiONPs respectively, and characterized with x-ray diffraction (XRD), and zeta potential (ZP); The average crystalline sizes computed were 11.57 nm and 13.36 nm for OPE/BiONPs and LPE/BiONPs respectively; The zeta potentials values were −36.8 mV, and −35.5 mV for OPE/BiONPs, and LPE/BiONPs respectively; Polyacrylonitrile (PAN) polymer and the BiONPs blends were electrospun into nanofibers to get unblended PAN nanofiber (NF), OPE/BiO NF, and LPE/BiO NF; Scanning electron microscopic (SEM) analysis was used to determine the morphology of the electrospun nanocomposites; The NF, the OPE/BiO NF, and LPE/BiO NF possessed average diameters of 833 ± 125, 282.86 ± 29, and 558.76 ± 81 nm respectively; The nanofibers were examined for their antimicrobial activities against five (5) pathogens of public health significance comprising Gram-positive (*Bacillus cereus* and *Enterococcus faecalis*) and Gram-negative (*Salmonella enteritidis, Escherichia coli, and Vibrio cholerae*) bacteria, using the standard dilution microplate-method; The synthesized nanomaterials showed various levels of inhibitory activities against the target pathogens. The LPE/BiO NPs exhibited 98% inhibition to the growth of *Enterococcus faecalis* at a concentration of 810 $\mu$g ml$^{-1}$, while OPE/BiO NPs showed 71% inhibition to the *Escherichia coli* at a concentration of 243 $\mu$g ml$^{-1}$. The LPE/BiONF had 72% inhibition of *S. enteritidis* at MIC of 2.7 mg ml$^{-1}$. The antimicrobial activities of CPE/BiONPs, LPE/BiONF and their NFCs could have a comparative advantage against commercial antibiotics and hence could be used in the control of waterborne pathogens.

## 1. Introduction

The presence of pathogens in drinking water could result in a major outbreak of diseases that could leave lethal effects on humans and the environment. About 1.6 million children die per annum consequent to disease outbreaks, of which polluted drinking water is the foremost cause [1]. According to WHO and UNICEF data, the consumption of contaminated water and poor sanitation in developing countries is the major cause of death of more than 2.2 million people per annum [2]. Microbial pathogens could contaminate the aquatic system, leading to various waterborne diseases. Furthermore, infectious and pathogenic diseases are threats to the life of approximately 60% of newborn babies [3].

The burden associated with waterborne disease in the United States was estimated at 1 billion USD and 12 billion USD globally annually. According to the projection by WHO, improvement in the quality of water could

reduce the burden of waterborne diseases globally by roughly 4%. Therefore, several strategies have been employed to overcome the problem of water pollution; One of the recent approaches exploited in water treatment is the use of nanoparticle composites with antimicrobial properties as nano-filters in replacement of the decontamination process through chlorination. Nanoparticles (NPs) are particulate dispersions or solid particles within the size range of 1 nm–100 nm [4].

The pursuit of green-mediated nanoparticle synthesis has resulted in the use of plant extracts, microorganisms or plant biomass in the synthesis as an eco-friendly substitute to the physical and chemical synthesis techniques that is conventionally used. Ali and co-workers employed *Aloe barbadensis* extract in the ZnO NPs synthesis, which showed an antibacterial properties against *S. aureus* and *E. coli* [5]. Copper and its complexes have been used in water purification, eliminating the growth of algae, fungi, and bacteria and reducing fouling [6]. Prakash and co-workers described the green synthesis of CuO NPs from plant and metal precursors of an aqueous extract *of Cordia sebestena* (*C. sebestena*) flower and copper nitrate respectively. The study demonstrated its promising applications as antimicrobials, photodegradation of Bractive T Blue (BTB), and Biginelli reaction. The bio-grown CuO NPs exhibited an absorption peak at 267 nm from the UV–vis spectroscopy, an agglomerated spherical shape having a particle diameter between 20–35 nm with crystallinity rising from FESEM-EDX analysis and TEM-SAED patterns. The zeta potential value of −26 mV portrays moderate stability. Their finding suggests that the CuO NPs possess antimicrobial activities against some environmental bacterial pathogens and could be used in photolysis to eliminate water pollutants [7]. Fuku and co-workers also reported the successful green synthesis of $Cu/Cu_2O/ZnO$ and their electrochemical behaviour towards ethanol production using pomegranate peels extract [8].

The preparation of Nanofibers (NFs) is done using different techniques, namely drawing [9], template synthesis [10, 11], phase separation [11], self-assembly [11, 12] and electrospinning [13, 14]; Electrospinning is reported to be the only technique that could enhanced the mass production of one-by-one continuous nanofibers from different polymers. It has also proven to be a powerful technique for fabricating polycrystalline polymer/ceramic [15] and single-crystalline ultrafine nanofibril bundles [16]; Diverse electrospun ZnO-based nanofiber mats have shown antimicrobial properties against a different range of bacterial strains [17–19]; However, the route of synthesis of the nanocomponents employed in fabricating the NFs has often involved the use of non-environmentally friendly matrices, and tedious in its approach.

Polyacrylonitrile (PAN) nanofibers (NFs) are considered one of the first three most fabricated fibres [20]. Their unique performance characteristics such as high thermal conductivity, resistance to ultraviolet light, high chemical resistance, and mechanical strength have attracted attention in the scientific community. Polyacrylonitrile is an affordable and commonly used engineering polymer. It is used in the conventional textile industry, in the production of customized army clothing [21], antibacterial and medical clothing [22], superhydrophobic surface finishes [10], as components of different forms of composites [23], used in electrical devices [24], optoelectronic, photonic devices [25], and energy storage systems [26]. Polyacrylonitrile possesses strong electrostatic characteristics which enhance the attraction of microbes and dust particles [27], and consequently, enjoys application in highly efficient dust-separating filters by getting rid of toxic compounds [28]. Additionally, the polymer has been exploited for various applications in diverse biosensors [29]. The PAN-derived membranes are famous for their high mechanical strength and thus can be used in membrane processes requiring resilience under pressure. The solubility of PAN in solvents and its ability to form a solution with solvents such as dimethyl sulfoxide (DMSO), dimethylformamide ( DMF), dimethylacetamide (DMA), dioxanone [30, 31], dimethyl sulfone, chloroacetonitrile, dimethyl phosphite, $\gamma$-butyrolactone, nitric acid, ethylene carbonate, and sulfuric acid has further amplified its functionalities and applications [32], thereby justifying its choice in this study.

The rising demands to reduce waste and utilise an environmentally friendly method in the derivation of compounds necessitates the use of agro-waste such as citrus peels in the green synthesis of functionalised materials in this study. In this work, we present the use of lemon and orange peels extract to reduce simultaneously copper and zinc precursor salts into $Cu_2O/ZnO$ NPs, and their fabrication into PAN-based nanofiber using electrospinning technology. The prepared bioxide NPs (BiONPs) and their PAN based nanofibers were investigated for their ability to inhibit the growth of five (5) pathogens of public health significance comprising Gram-positive and Gram-negative bacteria, using the standard dilution microplate method. This is the fifth paper in this series using orange and lemon peel extracts in nanotechnology.

## 2. Experimental procedures

### 2.1. Materials and characterization

Chemicals were purchased in their pure states, and hence no purification was required before use. Sigma-Aldrich, and SAARCHEM (South Africa), supplied the zinc and copper nitrates respectively that were used in the

study. The dissolution solvents N, N-Dimethylformamide (DMF) and Dimethyl sulfoxide (DMSO) were acquired from Emsure Iso (Germany) while Sodium hydroxide was purchased from Promark Chemicals (South Africa). Polyacrylonitrile (PAN; 150, 000 MW) and the standard culture microbes studied were also purchased from Sigma-Aldrich, South Africa.

The materials were characterized as detailed in our earlier reports [31, 32]. Briefly, Röntgen PW3040/60 X'Pert Pro x-ray diffractometer (Germany) was used to examine the crystallinity of the NPs synthesized. The Quanta FEG 250 environmental scanning electron microscopes (ThermoFisher Scientific, USA), and the Zeta sizer were respectively used to investigate the morphology and stability of the nanomaterials.

### 2.2. Synthesis of $Cu_2O$/ZnO NPs

The NPs were prepared following the steps reported in our previous works [31, 32]. Summarily, the metal salts ions were reduced with citrus peel extracts of orange and lemon in the presence of NaOH while stirring at temperature (T), where 60 °C < T °C < 100 °C. From our earlier reports [33, 34], citrus peels and some other plants have been used as both reducing, capping and stabilizing agents of the nanoparticles. In this synthesis, NaOH was added to catalyze and complex the reaction which on further heating, decomposes to its oxide. Hence the activity of the plant extracts with lower pH, as in the case of the citrus peel extract (pH < 5), was improved by the addition of the hydroxide ions [35].

### 2.3. Electrospinning of nanofibers

#### *2.3.1. Electrospinning of PAN nanofibers*

The, PAN was dried at 60 °C in an oven for about 24 h and collected in an airtight reagent bottle for further use. The dried PAN (12 wt%) was dissolved in DMF and stirred at room temperature for 64 h to get a clear solution. This was followed by stirring at 60 °C–70 °C for an additional 1 h to ensure complete dissolution of the polymer in the DMF. The mixture was fed into a 20 ml syringe, fitted into a programmable syringe pump electrospinning system. The PAN mixture was electrospun into a nanofiber at the tip-to-collector distance of 10 cm, at a flow rate of 0.02 ml $min^{-1}$ and positive potential of 30 kV. All the experimental procedures were carried out under static atmospheric conditions. The fabricated PAN-NFs were collected over aluminium covered metal plate collector, rid of DMF by drying at 100 °C in an oven, and subsequently kept in a cold and dry place for further characterization and application.

#### *2.3.2. Electrospinning of PAN nanocomposites*

About 8 mg of metal oxide (MO) NPs were introduced into 1 ml of DMSO and sonicated for about 2 h 30 min and was added to 5 ml of the prepared DMF-PAN mixture. The mixture was then stirred at room temperature overnight. The resultant mixture was sonicated for another 30 min to ensure smooth surfaced nanofibers. Using the same spinning parameters used to prepare the PAN-NF, the mixture was electrospun into nanofiber composite, and was designated as CPE/MO-NFs.

### 2.4. Antimicrobial studies

The antimicrobial activities of the nanomaterials were evaluated based on the minimum inhibitory concentrations (MIC) using the microdilution method as described by National Committee for Clinical Laboratory Standards (NCCLS 2000). The selected nanoparticles and nanocomposites were dissolved in DMSO to achieve a concentration of 30 mg $ml^{-1}$ and were tested against pathogens of public health significance (*Bacillus cereus, Salmonella enteritidis, Escherichia coli, Enterococcus faecalis and Vibrio cholerae*). A commercial antibiotic Ciprofloxacin (5 $\mu g\, g^{-1}$) was used as a positive control in the experiment while DMSO served as internal control and the nutrient broth was used as a negative control. Sterile 96-well microtitre plates were used for the assay. Test pathogens were grown overnight, and the concentration was adjusted to 0.5 McFarland ($1.5 \times 10^6$ CFU $ml^{-1}$) concentrations before use in the study. Sterile nutrient broth (100 $\mu l$) was dispensed into the micro-titre plates and appropriate equal concentrations of test pathogens (100 $\mu l$) were inoculated into the wells, after which the suspension containing 100 $\mu l$ of nanomaterials was transferred into the first well. A 3-fold dilution was made across the wells. The inoculated microtitre plates were then incubated at 37 °C for 24 h. The optical density (OD) of the cultures in micro-titre plates was measured at 630 nm in a UV-visible spectrophotometer after 24 h of incubation of bacterial cells. The minimal inhibitory concentration (MIC) of the nanomaterials against individual pathogens was determined as the lowest concentration of nanoparticles that caused inhibition of the pathogen.

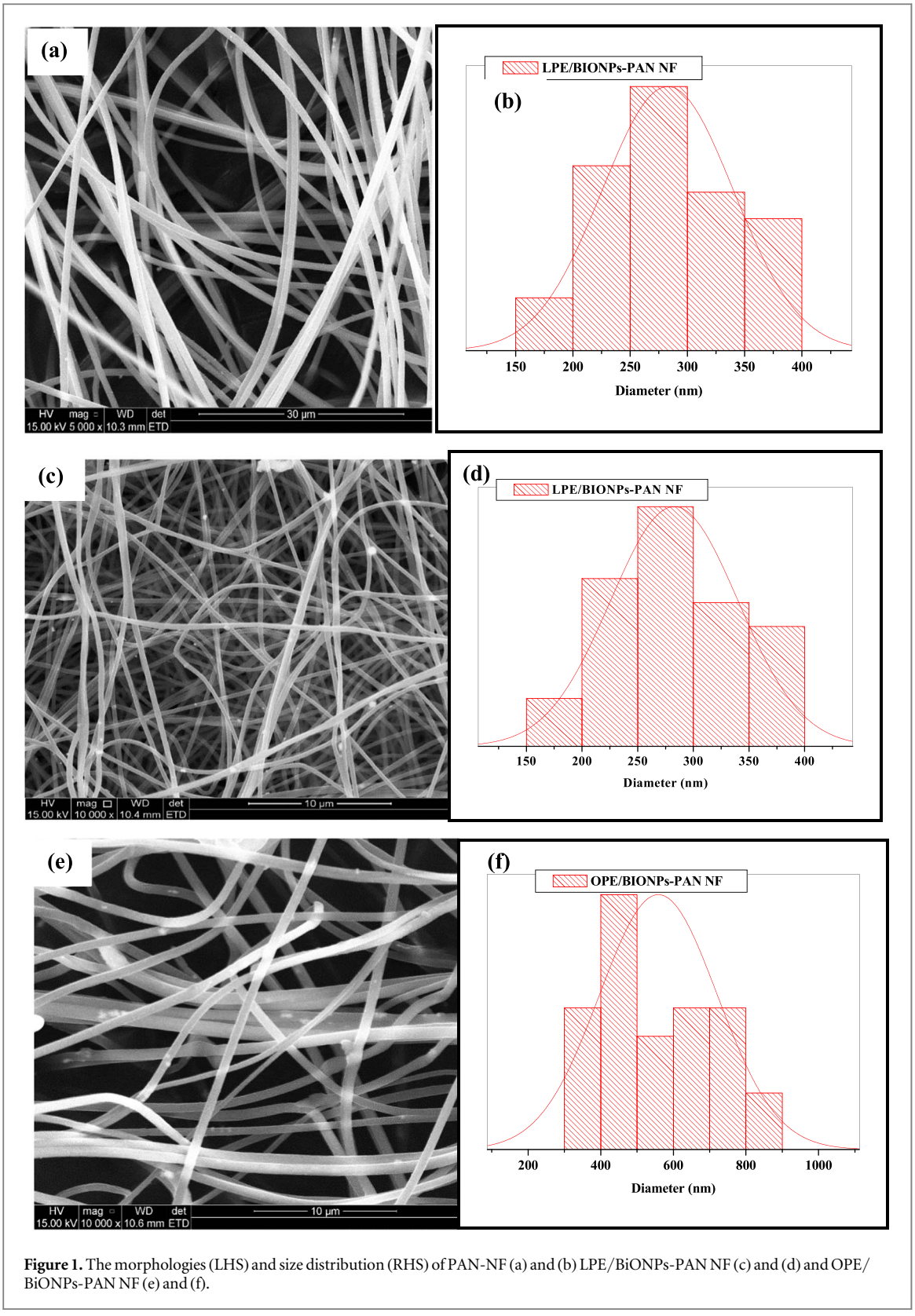


**Figure 1.** The morphologies (LHS) and size distribution (RHS) of PAN-NF (a) and (b) LPE/BiONPs-PAN NF (c) and (d) and OPE/BiONPs-PAN NF (e) and (f).

## 3. Results and discussion

### 3.1. Scanning electron microscopy (SEM)

The SEM images of the electrospun nanofiber composite (NFC) are represented in figure 1. The SEM micrographs of the NFC reveal that the fibre strands formed were roughly beadles with relatively similar diameter size distributions (table 1). The pure NF has the largest average diameter of 833 ± 125.00 nm, and the broadest size distribution of 444–1571 nm, while the LPE/BiONPs-PAN (LPE/BiO NF) has the lowest average

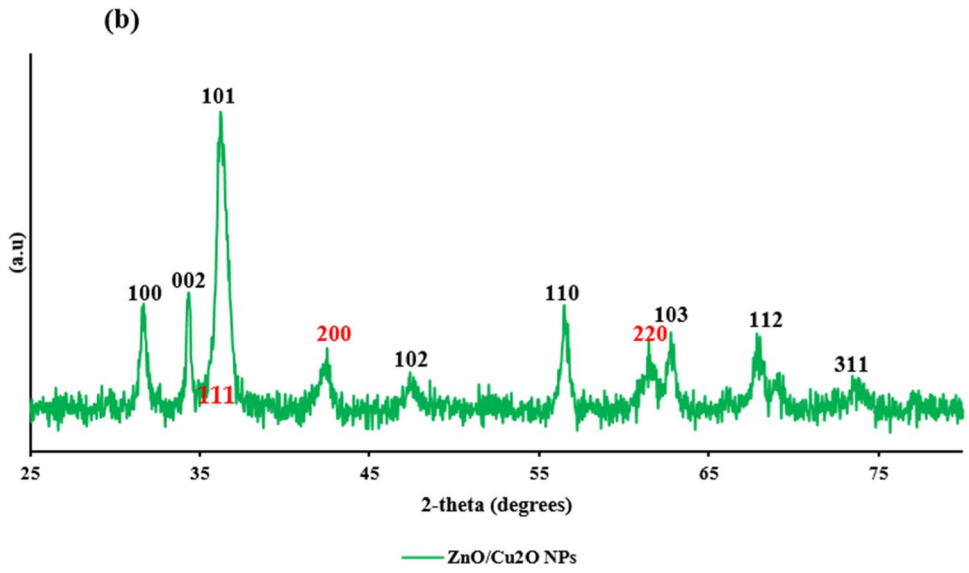


**Figure 2.** The XRD patterns (ZnO NPs-black; $Cu_2O$ NPs –red) of the (a) LPE/NPs and (b) OPE/NPs.

**Table 1.** The size distribution and size of NFC.

| NF | Distribution (nm) | Average (nm) | Beads |
|---|---|---|---|
| Pure PAN | 444–1571 | $833 \pm 125.00$ | none |
| LPE/BIONPS-PAN | 210–393 | $282.86 \pm 28.68$ | tiny |
| OPE/BIONPS-PAN | 306–894 | $558.76 \pm 81.17$ | negligible |

diameter ($282.86 \pm 28.68$ nm). The LPE NFC were generally less than 300 nm, while the OPE NFC was generally above 500 nm. Additionally, the inter-fibre spacing was more pronounced in the OPE NFC than in the LPE NFC; Experimentally, beyond the differences in the NPs precursor used to prepare the NF, the discrepancy in the diameters from the LPE and OPE citrus peels extracts could also be attributed to slight differences in the preparation of the NF mixture. To achieve a better viscosity of electrospinnable solution for the LPE NFC based PAN nanofiber, the solution was heated at a relatively higher temperature than that of the OPE NFC.

### 3.2. Zeta potential

Zeta potential ($\zeta$) is an essential tool for defining the charges on the surface of NPs in aqueous form and envisaging long-term stability [50]. The zeta values for the BiONPs of ZnO/$Cu_2O$/OPE, and ZnO/$Cu_2O$/LPE were −36.8 mV, and −35.3 mV respectively. These values confirm the very stable nature of the composite.

### 3.3. XRD

The XRD results of the BiONPs powdered samples signify the presence of ZnO and $Cu_2O$ in all the CPE as shown in figure 2. The $Cu_2O$ were characterized mainly with the planes of (111), (200) and (220) corresponding to diffraction peaks ($2\theta$) = 36.40°, 42.24° and 61.31° respectively (JCPDS card no: JPC2-05-0667-cuprite-$Cu_2O$) [31], while the ZnO NPs were characterized with the three planes (100), (002) and (101) corresponding to 2-theta ($2\theta$) of 31.81°, 34.55°and 36.20° respectively, (JCPDS card no. 36-1451 zincite) [32]. Hence, the BiONPs were indexed with the planes of (100), (101), (111), (200), and (220) corresponding to 2-theta ($2\theta$) of 31.8°, 36.20°, 36.40°, 42.24° and 61.31° respectively; The average crystallite size was estimated from the XRD peak width of the preferential plane (101) corresponding to 2-theta ($2\theta$) = 36.20°. With ZnO NPs having a more prominent intensity, using the same Debye–Scherrer equation [36], the average sizes of the BiONPs computed were 11.57 nm, and 13.36 nm for OPE/BiONPs, and LPE/BiONPs, respectively. These values are lower than the monometallic particles of ZnO NPs LPE (21.98 nm) and ZnO NPs OPE (18.49 nm) reported in our earlier work [34]. The smaller pattern of the BiONPs compared to the mono-NPs with the resultant broader diffraction peaks are consistent with earlier literature report [37]. However, this is not true for the $Cu_2O$ NPs monometallic-NPs that was, 8.03 nm and 9.0 nm in LPE/CuONPs and OPE/CuONPs respectively [33]; This may be due to the predominance of the ZnO NPs in the core–shell of BiONPs from the CPE. Assuming also a preferential formation of the ZnO NPs in the composite. The d-spacing and lattice constants are presented in table 2.

**Table 2.** Spacing of the planes (dhkl) from XRD, JCPDS data card for equivalent (h k l) planes and percentage of variations of a/c with JCPDS.

| Sample | a = b (Å) | c(Å) | c/a | d100(Å) | d002(Å) | d101(Å) | % *C |
|---|---|---|---|---|---|---|---|
| JCPDS | 3.2495 | 5.2066 | 1.6023 | 2.8141 | 2.6033 | 2.4757 | — |
| BiONPs/LPE | 3.2566 | 5.2162 | 1.6017 | 2.8203 | 2.6081 | 2.4809 | 0.0374 |
| BiONPs/OPE | 3.2596 | 5.2224 | 1.6022 | 2.8228 | 2.6112 | 2.4833 | 0.0062 |
| ZnO NPs/CPE | 3.2656 | 5.2095 | 1.5997 | 2.8202 | 2.6048 | 2.4803 | 0.1622 |

% *C: % of contraction in c/a with JCPDS.

**Table 3.** Codes for test samples considered and definition of abbreviations.

| S/N | Labels | Description |
|---|---|---|
| 1 | LPE/BiONPs | LPE-mediated BiO NPs |
| 2 | OPE/BiONPs | OPE-mediated BiO NPs |
| 3 | PAN NF | Pure PAN nanofiber |
| 4 | LPE/BiONPs/ PAN NF | LPE-mediated BiO NPs-PAN NF |
| 5 | OPE/BiONPs/ PAN NF | OPE-mediated BiO NPs-PAN NF |
| 6 | MxIC | Maximum inhibitory concentrations |
| 7 | MIC | Minimum inhibitory concentration |
| 8 | MxIE | Maximum inhibitory efficiency |
| 9 | MIE | Minimum inhibitory efficiency |
| 10 | ZP | Zeta potential |

**Table 4.** The antimicrobial activities of the nanocomposites against *E. coli*.

| Samples | MxIC ($\mu$g ml$^{-1}$) | MxIE (%) | MIC ($\mu$g ml$^{-1}$) | MIE (%) | Particle size (nm) | ZP (mV) | References |
|---|---|---|---|---|---|---|---|
| LBiONPs | 6.8 | 66.27 | 6.8 | 66.27 | 13.36 | −35.3 | This work |
| OBiONPs | 243 | 71.22 | 1.9 | 34.94 | 11.57 | −36.8 | This work |
| PAN | 810 | 39.09 | 6.8 | 24.97 | 833.00 | — | This work |
| LBiONF | 1.9 | 29.34 | 1.9 | 29.34 | 282.86 | — | This work |
| OBiONF | 6.8 | 28.96 | 1.9 | 19.68 | 558.76 | — | This work |
| PC | 3.2 | 72.55 | — | — | — | — | This work |
| PVA-Fe-ZnO NPs | — | 88 | — | — | 120–250 | — | [17] |
| ZnO-NPs | 31.25 | — | | — | 30 | — | [38] |
| ZnO-NPs | 500 | — | | — | 15 | | [39] |
| CuO-NPs | 500 | — | — | — | 22 | | [39] |

### 3.4. Antimicrobial activities of the nanocomposites

The antimicrobial activities of the nanomaterials listed below (table 3) were investigated against five (5) pathogens of public health significance comprising Gram-positive (*Enterococcus faecalis and Bacillus cereus*) and Gram-negative (*Salmonella enteritidis, Escherichia coli, and Vibrio cholerae*), using the standard dilution microplate-method. The average size of the NPs considered was between 11.57 nm and 13.36 nm, while that of the NFs is D (nm), where $200 < D < 900$ nm.

#### *3.4.1. E. coli*

The inhibitory activities of the prepared nanocomposites against the growth of *E. coli* are represented in table 4. The OPE/BiONPs resulted in the highest (maximum) inhibition efficiency of 71.22% (MxIE) at the maximum inhibitory concentration of 243 $\mu$g ml$^{-1}$. This performance is also comparable with LPE/BiONPs having a maximum inhibitory efficiency of 66.27% at a very low MIC of 6.8 $\mu$g ml$^{-1}$, and the positive control (ciprofloxacin) with maximum inhibitory efficiency of 72.55%. The minimum inhibition efficiency (MIE) of 19.68% at MIC of 1.9 $\mu$g ml$^{-1}$ was observed for OPE/BiONF against *E. coli*, followed by LPE/BiONF with MIE of 29.34%. The higher inhibition of these NPs relative to the NFC, against *E. coli* could be due to the faster access of smaller particle size of the 'free' NPs, thus enhancing the penetration into the microbial cells which could have

**Table 5.** The antimicrobial activities of the nanocomposites against *E. faecalis*.

| Samples | MxIC ($\mu$g ml$^{-1}$) | MxIE (%) | MIC ($\mu$g ml$^{-1}$) | MIE (%) | Particle size (nm) | ZP (mV) | References |
|---|---|---|---|---|---|---|---|
| LBiONPs | 810 | 98.29 | 1.9 | 5.94 | 13.36 | −35.3 | This work |
| OBiONPs | 810 | 41.68 | 6.8 | 16.43 | 11.57 | −36.8 | |
| PAN | 810 | 29.5 | 243 | 1.98 | 833.00 | — | |
| LBiONF | 9000 | 80.85 | 6.8 | 45.85 | 282.86 | — | |
| OBiONF | 240 | 30.66 | 1.9 | 2.56 | 558.76 | — | |
| PC | 12.15 | 90.07 | 1.9 | 73.51 | — | — | — |
| ZnO-NPs | 500 | — | — | — | 15 | — | [39] |
| CuO-NPs | 500 | — | — | — | 22 | — | [39] |
| ZnO-NPs | 1000 | — | — | — | 20–50 | — | [39] |

**Table 6.** The Antimicrobial Activities of the Nanocomposites against *S. enteritidis*.

| Samples | MxIC ($\mu$g ml$^{-1}$) | MxIE (%) | MIC ($\mu$g ml$^{-1}$) | MIE (%) | Particle size (nm) | ZP (mV) | References |
|---|---|---|---|---|---|---|---|
| LBiONPs | 243 | 62.31 | 240 | 62.31 | 13.36 | −35.3 | This work |
| OBiONPs | — | — | — | — | 11.57 | −36.8 | This work |
| PAN | 72.9 | 94.78 | 1.9 | 13.55 | 833.00 | — | This work |
| LBiONF | 9000 | 83.82 | 2700 | 72 | 282.86 | — | This work |
| OBiONF | 243 | 83.21 | 72.9 | 0.8 | 558.76 | — | This work |
| PC | 405 | 99.22 | 3.17 | 91.45 | — | — | This work |
| AgNPs | — | — | 0.313 | 23.13 | $6.8 \pm 2.28$ | $-37.3 \pm 5.7$ | [45] |
| $TiO_2$ NPs | $2500 \pm 0.2$ | — | — | — | 10 ~ 25 | — | [46] |
| ZnO NPs | $3000 \pm 0.2$ | — | — | — | ~20 | — | [46] |

destroyed the DNA, thus hampered its cell replication, and eventually resulting into cellular death. The antimicrobial activities of the nanomaterials also show inverse relation with their sizes. This trend agrees with earlier reports by Azam [36, 37]. The MIC reported here for CPE/BiONPs, is much lower than that reported by Alekish, Ismail [38], for ZnO-NPs against *E. coli*. All the NFCs counterparts however demonstrated less than 90% inhibition.

*3.4.2. E. faecalis*

In table 5, the antimicrobial activities of the synthesized nanomaterials against the growth and multiplication of *E. faecalis* are presented. The LPE/BiONPs resulted in a very high inhibition efficiency (98.29%) against *E. faecalis,* at a maximum inhibitory concentration (MxIC) of 810 $\mu$g ml$^{-1}$. At a very low concentration of 1.9 $\mu$g ml$^{-1}$, LBiONPs inhibited the growth of *E. faecalis* (5.94%). At the MxIC of 810 $\mu$g ml$^{-1}$, OPE/BiONPs offered a maximum inhibition of 41.68% and a minimum inhibition concentration (MIC) of 1.9 $\mu$g ml$^{-1}$ against *E. faecalis* at an efficiency of 16.43%. The PAN-NF also demonstrated a capacity for antimicrobial activity with a maximum inhibitory efficiency of approximately 30% at 810 $\mu$g ml$^{-1}$, and negligible inhibition at the MIC of 1.9 $\mu$g ml$^{-1}$. The LBiONF showed a great improvement in the antibacterial activity of the PAN with more than 80% inhibition at 9 mg ml$^{-1}$, while the addition of OPE/BiO NPs did not improve the antimicrobial activities of OPE/BiONF against *E. faecalis*. The synergy between the synthesized LPE/BiONPs and its nanofibre of LPE/BiONF could be responsible for the improved inhibitory activities of the LPE/BiONF composite. The LPE/BiONPs with larger particle size than the OPE/BiONPs, have higher inhibition efficiency against *E. faecalis* at MIC of 810 $\mu$g ml$^{-1}$. This trend nonetheless, contradicts the earlier reports of Shinde [40], Azam, Ahmed [41]. This, however, is not unlikely, considering the zeta potential values of the NPs. Chang, Lin [42] asserted that particles with more negative zeta potential value, are likely to have lower antimicrobial activities amidst other factors. As expected, the commercial antibiotic had a higher inhibition of *E. faecalis* at a very low MIC compared to CPE/BiONPs.

*3.4.3. S. enteritidis*

The inhibitory activities of the nanomaterials against the growth and multiplication of *S. enteritidis* are shown in table 6. Most of the designed materials performed relatively better in inhibiting *S. enteritidis*. The LBiONPs showed maximum inhibitory efficiency of 62.31% at the MxIC of 240 $\mu$g ml$^{-1}$, while the counterpart OPE/BiONPs could not resist the growth of the pathogens for all the range of concentrations investigated. At a very low MxIC of 72.9 $\mu$g ml$^{-1}$, the Pure PAN NF resulted in approximately MxIE of 95% inhibition and MIE of 13.55% (at MIC of 1.9 $\mu$g ml$^{-1}$) to the growth and multiplication of *S. enteritidis.* Meanwhile, the NFC did better

**Table 7.** The Antimicrobial Activities of the Nanocomposites against *V. cholerae*.

| Samples | MxIC ($\mu$g ml$^{-1}$) | MxIE (%) | MIC ($\mu$g ml$^{-1}$) | MIE (%) | Particle size (nm) | ZP (mV) | References |
|---|---|---|---|---|---|---|---|
| LBiONPs | 243 | 64.5 | 1.9 | 40.3 | 13.36 | −35.3 | This work |
| OBiONPs | 810 | 49.15 | — | — | 11.57 | −36.8 | This work |
| PAN | — | — | — | — | 833.00 | — | This work |
| LBiONF | 2700 | 75 | 1.9 | 35.35 | 282.86 | — | This work |
| OBiONF | 243 | 14.7 | 1.9 | 11.60 | 558.76 | — | This work |
| PC | 3.16 | 93.82 | — | — | — | — | This work |
| ZnO NPs | | | 25 | — | 1–100 | | [45] |
| $AgNO_3$ | | | 20 | | >1000 | | [46] |
| AgNPs | | | 10 | | 20–30 | | [46] |

**Table 8.** The Antimicrobial Activities of the Nanocomposites against *B. cereus*.

| Samples | MxIC ($\mu$g ml$^{-1}$) | MxIE (%) | MIC ($\mu$g ml$^{-1}$) | MIE (%) | Particle size (nm) | ZP (mV) | References |
|---|---|---|---|---|---|---|---|
| LBiONPs | — | — | — | — | 13.36 | −35.3 | This work |
| OBiONPs | 810 | 61.28 | | | 11.57 | −36.8 | This work |
| PAN | 6.8 | 53.82 | — | — | 833.00 | — | This work |
| LBiONF | — | — | — | — | 282.86 | — | This work |
| OBiONF | 72.9 | 58.49 | 1.9 | 16.01 | 558.76 | — | This work |
| PC | 3.17 | 92.51 | 3.17 | 56.4 | — | — | This work |
| $Fe_3O_4$-NP | — | — | 40 | 40–50 | 24 | | [47] |

than the NPs but underperformed compared to the inhibitory activities of the pure NF. At the MxIC of 9 mg ml$^{-1}$ and 243 $\mu$g ml$^{-1}$, the LPE/BiONF and OPE/BiONF offered more than 80% inhibition respectively, to the growth of the target pathogen. Interestingly, at MIC of 2.7 mg ml$^{-1}$, the LPE/BiONF had 72% inhibition of *S. enteritidis*. As expected, the positive control, had higher percent inhibition than the prepared nanomaterials. This result correlates with the MIC of silver NPs in the earlier report of Farouk, El-Molla [43], on the antimicrobial activities of silver NPs against antibiotics resistant *S. enteritidis* strain. Alizadeh-Sani [44] reported a MIC of 3.00 ± 0.21 mg ml$^{-1}$ for ZnO, and 2.50 ± 0.17 mg ml$^{-1}$ for $TiO_2$ against the growth of *S. enteritidis*. These data put the antimicrobial activities of CPE/BiONPs and their NFCs at a comparative advantage and, could hence have applications in the control of waterborne pathogens.

### *3.4.4. V. cholerae*

*V. cholerae*, is a Gram-negative bacterium and did not show high susceptibility to the nanomaterials prepared in this study as observed in table 7. lBiONPs and the corresponding NF composite only had 64.5% at 243 $\mu$g ml$^{-1}$ and 75% at 2700 $\mu$g ml$^{-1}$ inhibition of *V. cholera*. Nonetheless, at low MIC (1.9 $\mu$g ml$^{-1}$), there was an inhibitory action of LBiONPs, LBiONF and OBiONF against *V. cholera*. The positive control as seen in table 7, did inhibit microbial growth more than the prepared materials. The inhibitory effect of metal oxides was also examined against *V. cholerae* by Raj [45] and Krishnaraj [46] and showed comparable antimicrobial activities with the present work. The data from the antimicrobial activities from the LBiONPs and the corresponding NF showed an advisable application in the control of *V. cholerae*.

### *3.4.5. B. cereus*

The antimicrobial activities of the OBiONPs substrate with more negative ZP values and smaller particle-sized seem to be better than their counterpart in this study. The LBiONPs offered no resistance to the growth of *B. cereus* either as NPs and NF composites (see table 8). At the MxIC of 810 $\mu$g ml$^{-1}$, and 79.2 $\mu$g ml$^{-1}$, the OBiONPs and OBiONF counterparts inhibited the growth of the *B. cereus* by 61.28% and 58.49% respectively. Positive control offered a MxIE of 92.51% at MIC of 3.17 $\mu$g ml$^{-1}$. A similar work by Ansari [47] showed a similar inhibition efficiency at a very low concentration.

### *3.4.6. Mechanism of antimicrobial activity of the nanomaterials*

The mechanism of the bactericidal effect of nanomaterial against bacteria remains quite unclear [48, 49]. However, this study affirms that the nanomaterials have antimicrobial activities against the public health significant pathogens and was comparable to the conventional antimicrobial agents employed in treating bacterial infections. These agents could have exhibited antimicrobial activities by interfering with the synthesis

of the cell walls or impairs pathogens protein and nucleic acid synthesis and replications process or altered the metabolic pathway of pathogen growth and virulence activities [49].

The study by Meghana, Kabra [50] had suggested that the antimicrobial activities of copper oxide nanoparticles are dependent on their oxidation states and could be toxic to *E. coli* when in their oxidative state. $Cu_2O$ could have promptly deactivated Fumarase A genes, an iron sulphur cluster enzyme thereby binding to the proteins. Therefore, CuO NPs antibacterial activities could be linked to the quick debility in the integrity of cell membranes and the generation of reactive oxygen species (ROS) [51]. It is proposed that within bacterial cells, sulfhydryl reduced Cu(II) ions to cuprous Cu(I) ions, which in turn are responsible to cause oxidative stress through Cu(I)—driven ROS [52]. The discharge of Cu ions from the surface of metallic Cu has also been proposed as the cause of its antimicrobial action [53]. Similarly, copper oxides could leach various copper salts in their microns and nano-dimensioned oxides, leading to bactericidal effects [54].

On the other hand, previous antimicrobial behaviour studies of zinc oxide NPs have revealed that the size, abrasiveness, surface roughness and defects, and oxidative stress play significant functions in the antibacterial activities of nanomaterials [40, 55, 56]. The antimicrobial activity of the NFCs has been attributed to the release of the NPs into the solution of the composite [57] which forms interaction site between the hybrid composite and the pathogen [58] as observed in CPE metal oxides NFCs in this study. Therefore, the integration of the CuO NPs or ZnO NPs and amine functional groups in the mat resulted in bacteriocidal activities against the bacterial pathogen.

Moreover, the CPE/MONPs deposition on the surface of the PAN nanofiber membrane results in an attachment to the cell membrane which allows for permeation into the cell, thereby attacking the genetic materials in the nucleus resulting in cell death. The generation of $H_2O_2$ from the catalytic process of CPE/MONPs, could have amplified the antibacterial activity against the test pathogens [59, 60]. CPE/MONPs have the ability to neutralize the surface potential of the bacterial cell thereby resulting in the generation of pairs of electron-hole which boosts ROS production that in turn kills the bacteria cell.

Therefore, CPE/MONPs could act as bacteriostatic agents with positive charges against negatively charged bacteria [61]. The resulting strong electrostatic interaction between the positively charged $Cu^{2+}$ or $Zn^{2+}$ions and the electronegative cell wall surface of the microbe could lead to damage in the phospholipid's molecular structure and consequently cause damage to the microbial cell membrane [62, 63]. In summary, the binding of nanoparticles to the surface of the cell surface is likely the most crucial moment that instigates a series of events that could lead to interruption and damage to cellular structures. In this work, however, as in most literature [50], the exact mechanism pathway for the antimicrobial activities of the nanomaterials was not determined, hence, the antimicrobial activities of the nanomaterials are comparable to that of earlier reports by previous authors [40, 58, 64]. However, this study provides information on the antimicrobial potentials of a green synthesized nanomaterials from citrus peel extract.

## 4. Conclusion

Bioxide NPs were prepared for bio-reduction copper and zinc salt solutions using extracts from orange and lemon peels. The prepared NPs from lemon peel extract (LPE/BiONPs) and orange peel extract (OPE/BiONPs) were characterized using XRD and zeta potential analysis. The LPE/BiONPs and OPE/BiO NPs were crystalline in sizes, likewise OPE/BiONPs, and LPE/BiONPs had stable zeta potential in the magnitude of −36.8 mV and −35.5 mV respectively. The plain LPE/BiO NF and OPE/BiO NF possessed size distributions between 444–1571 nm, 210–393 nm, and 306–894 nm. The fabricated NPs blended with PAN polymer and electrospun into nanofibers (LPE/BiO NF and OPE/BiO NF demonstrated antimicrobial activities against the growth of *B*acillus cereus*, Salmonella enteritidis, Escherichia coli, Enterococcus faecalis and Vibrio cholerae.*

## Data availability statement

All data that support the findings of this study are included within the article (and any supplementary files).

## Author contributions

O.E.F. conceptualized and designed the work and was part of the manuscript write-up. C.E.O, and S.A.A was involved in the manuscript preparation. All the authors reviewed the manuscript and agreed to publication.

## Funding

This research was funded by the National Research Foundation of South Africa for Thuthuka funding for Researchers (UID: 117709). The APC was funded by Higher Degree of North-West University, South Africa.

## Conflicts of interest

The authors declare no conflict of interest.

## Acknowledgments

CEO, SAA, and OEF thank the North-West University and MaSIM for their financial support and research facilities. OEF acknowledges the FRC of North-West University and the National Research Foundation of South Africa for Thuthuka funding for Researchers (UID: 117709).

## ORCID iDs

Enyioma C Okpara https://orcid.org/0000-0002-5884-3882
Omolola E Fayemi https://orcid.org/0000-0002-0049-5184

## References

[1] Fernandez-Luqueno F *et al* 2013 Heavy metal pollution in drinking water-a global risk for human health: A review *Afr. J. Environ. Sci. Technol.* **7** 567–84
[2] Azizullah A *et al* 2011 Water pollution in Pakistan and its impact on public health—a review *Environ. Int.* **37** 479–97
[3] Ullah R *et al* 2009 Assessment of groundwater contamination in an industrial city, Sialkot, Pakistan *Afr. J. Environ. Sci. Technol.* **3** 429–46
[4] Xia Y *et al* 2011 Chiral inorganic nanoparticles: origin, optical properties and bioapplications *Nanoscale* **3** 1374–82
[5] Ali K *et al* 2016 Aloe vera extract functionalized zinc oxide nanoparticles as nanoantibiotics against multi-drug resistant clinical bacterial isolates *J. Colloid Interface Sci.* **472** 145–56
[6] Perelshtein I *et al* 2009 CuO–cotton nanocomposite: Formation, morphology, and antibacterial activity *Surf. Coat. Technol.* **204** 54–7
[7] Prakash S *et al* 2018 Green synthesis of copper oxide nanoparticles and its effective applications in Biginelli reaction, BTB photodegradation and antibacterial activity *Adv. Powder Technol.* **29** 3315–26
[8] Fuku X *et al* 2020 Green synthesis of Cu/Cu2O/CuO nanostructures and the analysis of their electrochemical properties *SN Applied Sciences* **2** 1–15
[9] Ondarcuhu T *et al* 1998 Drawing a single nanofibre over hundreds of microns *EPL (Europhysics Letters)* **42** 215
[10] Feng L *et al* 2002 Super-hydrophobic surface of aligned polyacrylonitrile nanofibers *Angew. Chem. Int. Ed.* **41** 1221–3
[11] Martin C R 1996 Membrane-based synthesis of nanomaterials *Chem. Mater.* **8** 1739–46
[12] Whitesides G M *et al* 2002 Self-assembly at all scales *Science* **295** 2418–21
[13] Deitzel J M *et al* 2001 Controlled deposition of electrospun poly (ethylene oxide) fibers *Polymer* **42** 8163–70
[14] Fong H 2001 Electrospinning and the formation of nanofibers *Structure Formation in Polymeric Fibers* 225–46
[15] Dzenis Y 2004 Spinning continuous fibers for nanotechnology *Science* **304** 1917–9
[16] Li J-M 2017 Realizing single-crystalline vertically-oriented and high-density electrospun nanofibril bundles by controlled postcalcination *CrystEngComm* **19** 3392–7
[17] Sekar A D *et al* 2019 Electrospinning of Fe-doped ZnO nanoparticles incorporated polyvinyl alcohol nanofibers for its antibacterial treatment and cytotoxic studies *Eur. Polym. J.* **118** 27–35
[18] Jatoi A W *et al* 2019 Characterizations and application of CA/ZnO/AgNP composite nanofibers for sustained antibacterial properties *Mater. Sci. Eng. C* **105** 110077
[19] Hwang S H *et al* 2011 Electrospun ZnO/TiO 2 composite nanofibers as a bactericidal agent *Chem. Commun.* **47** 9164–6
[20] Bhanu V *et al* 2002 Synthesis and characterization of acrylonitrile methyl acrylate statistical copolymers as melt processable carbon fiber precursors *Polymer* **43** 4841–50
[21] Gibson P *et al* 2001 Transport properties of porous membranes based on electrospun nanofibers *Colloids Surf., A* **187** 469–81
[22] Lala N L *et al* 2007 Fabrication of nanofibers with antimicrobial functionality used as filters: protection against bacterial contaminants *Biotechnol. Bioeng.* **97** 1357–65
[23] Kim C *et al* 2007 Synthesis and characterization of porous carbon nanofibers with hollow cores through the thermal treatment of electrospun copolymeric nanofiber webs *Small* **3** 91–5
[24] Peng M *et al* 2006 Nanoporous structured submicrometer carbon fibers prepared via solution electrospinning of polymer blends *Langmuir* **22** 9368–74
[25] Yang Y *et al* 2007 Electrospinning of carbon/CdS coaxial nanofibers with photoluminescence and conductive properties *Materials Science and Engineering: B* **140** 48–52
[26] Im J S *et al* 2008 The study of controlling pore size on electrospun carbon nanofibers for hydrogen adsorption *J. Colloid Interface Sci.* **318** 42–9
[27] Hwang J-J *et al* 2012 Preparation, morphology, and antibacterial properties of polyacrylonitrile/montmorillonite/silver nanocomposites *Mater. Chem. Phys.* **136** 613–23
[28] Shim W G *et al* 2006 Adsorption characteristics of benzene on electrospun-derived porous carbon nanofibers *J. Appl. Polym. Sci.* **102** 2454–62

[29] Dhand C et al 2011 Recent advances in polyaniline based biosensors Biosens. Bioelectron. 26 2811–21
[30] Nouzaki K et al 2002 Preparation of polyacrylonitrile ultrafiltration membranes for wastewater treatment Desalination 144 53–9
[31] Kim I-C et al 2002 Preparation of asymmetric polyacrylonitrile membrane with small pore size by phase inversion and post-treatment process J. Membr. Sci. 199 75–84
[32] Wypych G 2016 PA-6 polyamide-6 Handbook of Polymers 2nd ed. (Toronto, ON, Canada: ChemTec Publishing) 215–20
[33] Okpara E C et al 2019 Comparative study of spectroscopic and cyclic voltammetry properties of CuONPs from citrus peel extracts Mater. Res. Express 6 105056
[34] Okpara E C et al 2020 Green wastes mediated zinc oxide nanoparticles: synthesis, characterization and electrochemical studies Materials 13 4241
[35] Wisam J A et al 2018 A novel study of pH influence on Ag nanoparticles size with antibacterial and antifungal activity using green synthesis World Scientific News 97 139–52
[36] Azam A et al 2010 Formation and characterization of ZnO nanopowder synthesized by sol–gel method J. Alloys Compd. 496 399–402
[37] Murugavelu M et al 2017 Synthesis, characterization of Ag-Au core–shell bimetal nanoparticles and its application for electrocatalytic oxidation/sensing of l-methionine Mater. Sci. Eng. C 70 656–64
[38] Alekish M et al 2018 In vitro antibacterial effects of zinc oxide nanoparticles on multiple drug-resistant strains of Staphylococcus aureus and Escherichia coli: An alternative approach for antibacterial therapy of mastitis in sheep Veterinary World 11 1428
[39] Reyes-Torres M A et al 2019 Synthesis of CuO and ZnO nanoparticles by a novel green route: antimicrobial activity, cytotoxic effects and their synergism with ampicillin Ceram. Int. 45 24461–8
[40] Shinde S S 2015 Antimicrobial activity of ZnO nanoparticles against pathogenic bacteria and fungi Sci Med Central 3 1033
[41] Azam A et al 2012 Antimicrobial activity of metal oxide nanoparticles against Gram-positive and Gram-negative bacteria: a comparative study Int. J. Nanomed. 7 6003
[42] Chang S-H et al 2015 pH Effects on solubility, zeta potential, and correlation between antibacterial activity and molecular weight of chitosan Carbohydrate Polym. 134 74–81
[43] Farouk M M et al 2020 The role of silver nanoparticles in a treatment approach for multidrug-resistant salmonella species isolates Int. J. Nanomed. 15 6993
[44] Alizadeh-Sani M et al 2020 Kinetics analysis and susceptibility coefficient of the pathogenic bacteria by titanium dioxide and zinc oxide nanoparticles Advanced Pharmaceutical Bulletin 10 56
[45] Agarwal H et al 2018 Mechanistic study on antibacterial action of zinc oxide nanoparticles synthesized using green route Chem. Biol. Interact. 286 60–70
[46] Krishnaraj C et al 2010 Synthesis of silver nanoparticles using Acalypha indica leaf extracts and its antibacterial activity against water borne pathogens Colloids Surf., B 76 50–6
[47] Ansari S A et al 2017 Antibacterial activity of iron oxide nanoparticles synthesized by co-precipitation technology against Bacillus cereus and Klebsiella pneumoniae Polish Journal of Chemical Technology 19 110–5
[48] Padmavathy N et al 2008 Enhanced bioactivity of ZnO nanoparticles—an antimicrobial study Sci. Technol. Adv. Mater. 9 035004
[49] Guzman M et al 2012 Synthesis and antibacterial activity of silver nanoparticles against gram-positive and gram-negative bacteria Nanomed. Nanotechnol. Biol. Med. 8 37–45
[50] Meghana S et al 2015 Understanding the pathway of antibacterial activity of copper oxide nanoparticles RSC Adv. 5 12293–9
[51] Jadhav S et al 2011 Copper oxide nanoparticles: synthesis, characterization and their antibacterial activity J. Cluster Sci. 22 121–9
[52] Ren J et al 2011 Crystallography facet-dependent antibacterial activity: the case of Cu2O Ind. Eng. Chem. Res. 50 10366–9
[53] Gunawan C et al 2011 Cytotoxic origin of copper (II) oxide nanoparticles: comparative studies with micron-sized particles, leachate, and metal salts ACS Nano 5 7214–25
[54] Midander K et al 2009 Surface characteristics, copper release, and toxicity of nano-and micrometer-sized copper and copper (II) oxide particles: a cross-disciplinary study Small 5 389–99
[55] Stoimenov P K et al 2002 Metal oxide nanoparticles as bactericidal agents Langmuir 18 6679–86
[56] Wang X et al 2007 A study on the antibacterial activity of one-dimensional ZnO nanowire arrays: effects of the orientation and plane surface Chem. Commun. 42 4419–21
[57] Pan S-F et al 2018 Synthesis of silver nanoparticles embedded electrospun PAN nanofiber thin-film composite forward osmosis membrane to enhance performance and antimicrobial activity Ind. Eng. Chem. Res. 58 984–93
[58] Shalaby T et al 2018 Electrospun nanofibers hybrid composites membranes for highly efficient antibacterial activity Ecotoxicology And Environmental Safety 162 354–64
[59] Dutta R K et al 2010 Differential susceptibility of Escherichia coli cells toward transition metal-doped and matrix-embedded ZnO nanoparticles J. Phys. Chem. B 114 5594–9
[60] Munnawar I et al 2017 Synergistic effect of Chitosan-Zinc Oxide Hybrid Nanoparticles on antibiofouling and water disinfection of mixed matrix polyethersulfone nanocomposite membranes Carbohydrate Polym. 175 661–70
[61] Unuabonah E I et al 2017 Novel metal-doped bacteriostatic hybrid clay composites for point-of-use disinfection of water J. Environ. Chem. Eng. 5 2128–41
[62] Motshekga S C et al 2018 Synthesis and characterization of alginate beads encapsulated zinc oxide nanoparticles for bacteria disinfection in water J. Colloid Interface Sci. 512 686–92
[63] Rajavel K et al 2014 In vitro bacterial cytotoxicity of CNTs: reactive oxygen species mediate cell damage edges over direct physical puncturing Langmuir 30 592–601
[64] Yoon K-Y et al 2007 Susceptibility constants of Escherichia coli and Bacillus subtilis to silver and copper nanoparticles Sci. Tot. Env. 373 572–5